J MATER SCI **41** (2006) 377–382

Thermally stimulated discharge current and DC resistivity of ethylene propylene rubber with various Pb concentrations

FANGGAO CHANG[*]
College of Physics & Information Engineering, Henan Normal University, Xinxiang 453002, Henan Province, People's Republic of China
E-mail: chfg@henannu.edu.cn

TIEPAN LI
Department of Physics, Henan Institute of Education, Zhengzhou 450014, Henan Province, People's Republic of China

DC resistivity of extruded ethylene propylene rubber (EPR) samples with various Pb concentration have been measured under wet conditions as a function of electrical field at selected temperatures in a range from 20 to 100°C. The temperature and electrical field coefficients of resistivity have been calculated. Thermally stimulated discharge current (TSDC) has also been measured and a broad positive peak has been observed for three EPR samples. It has been found that the resistivity of EPR is not sensitive to the Pb concentration within the range of 0 to 5 parts per hundred base resin (phr). The results show that the resistivity of EPR varies non-linearly with both temperature and electrical field. The temperature coefficient of resistivity α of EPR has been measured to be $\sim$0.1 K^{-1} for all the samples with various Pb concentration. The electrical field coefficient of resistivity β of EPR at room temperature is small and increases with temperature. Increasing Pb content increases slightly the electrical field coefficient β of resistivity. Based on a space charge limited conduction model, the trap depth of EPR has been estimated. TSDC measurements indicate that doping with Pb increases both the density of charge carriers and the number of deep traps simultaneously. The broad TSDC peak reveals that there must be a distribution rather than just a single value of the trap depth.

1. Introduction

Ethylene-propylene rubbers (EPR) and elastomers (also called EPDM and EPM) continue to be one of the most widely used and fastest growing synthetic rubbers having both specialty and general-purpose applications. In particular, EPR has been widely used in high voltage cable industry for number of years [1, 2]. In addition to its high electrical resistivity and breakdown strength, it has the advantage of more mechanical flexibility and higher water resistivity over other insulation materials, which makes it an ideal subsea insulation material [3–6]. Inclusion of filler, typically at 60 parts per hundred base resin (phr), improves the mechanical properties of EPR without reducing its electrical resistivity significantly. Red lead, Pb, is one of the components of the EPR formulation and is thought to impact improved electrical performance in wet conditions [7]. Although there have been extensive investigations on the physical properties of this commercially important polymer, little work has yet carried out concerning the effect of lead concentration on the electrical behaviour of EPR under wet conditions.

DC resistivity of an insulating material at a given temperature is a technologically important parameter. Many of the electrical designs require the knowledge of temperature dependence of resistivity. Furthermore, the resistivity of polymeric insulating materials such as EPR is in general varies with electrical field (also called electrical stress in electrical engineering). Measurements of temperature and electrical field dependences of resistivity of EPR provide not only the value of resistivity but also its

---

[*] Author to whom all correspondence should be addressed.

0022-2461 © *2006 Springer Science + Business Media, Inc.*
DOI: 10.1007/s10853-005-2572-9

temperature and field coefficients, which are essential to many high voltage electrical applications.

Introducing conductive Pb particles would in general reduce the resistivity of EPR. However, these particles may also create electron traps that would lead to a decrease in charge carrier mobility and hence increase the resistivity. Using thermally stimulated discharge current (TSDC) technique, the influence of chemical impurities that lead to the capture of charge carriers in electron traps can be studied with high sensitivity. TSDC method also provides information on the mechanism of electrical conductivity of polymers; it can also lead to a better understanding of the long-lived electrostatic charging of polymeric materials, which is due to the charge storage in electron traps.

In this paper we study the effect of Pb concentration on the electrical properties of EPR, by measuring the temperature and electrical field dependences of DC resistivity, and the thermally stimulated discharge current of EPR insulating materials under wet conditions.

2. Experimental

Pure elastomers are rarely used in technological applications. To provide particular required attributes, it is usual for them to be compounded with a number of additives. The formulation of the elastomeric compound studied here is based on an ethylene propylene hexadiene terpolymer including 66% (by weight) low-density ethylene and 22% clay: the stabilisation package forms less than 6%. The EPR materials with different Pb concentrations were supplied by Petrochemical Co. Ltd.

To measure the DC resistivity and the thermally stimulated discharge current, EPR materials with Pb concentration of 0, 2.5 and 5 phr respectively were extruded on to copper wires of 1 mm in diameter, using a conventional commercial production line. Five meters extruded wire, with a typical wall thickness of 1 mm, was immersed in a glass jar filled with tap-water. One end of the wire was connected to a Glassman high voltage unit capable of generating DC voltages up to 15 kV. The other end of the wire was left free in the air. The water in the glass jar acted as another electrode. As the resistivity of tap-water is roughly 8 orders smaller than that of the EPR insulating material, the resistance of water can be ignored in data processing.

The glass jar, together with the extruded wire sample was placed in a Grant W14 oil bath, with which the sample temperature can be increased up to 150°C. A K-type thermocouple was immersed in the water to measure the temperature to an accuracy of $\pm 0.1^\circ$C. The DC current across the extruded wire insulation was measured using a Keithly 617 programmable electrometer, which has a resolution of 10^{-16} A. The DC voltage output of the Glassman unit was controlled proportionally from zero to full scale by a 0–10 V DC signal supplied by the electrometer, and was monitored using a Black Star multimeter.

After a DC test voltage is applied to the sample, the current normally decays to a steady or quasi-steady value. The time to reach the steady state depends on the temperature, Pb concentration and electrical field. In the present work, current measurements were taken 60 s after a voltage step had been applied to the sample.

3. Results and discussion

3.1. The resistivity and its temperature and electrical field coefficients of EPR insulations with different Pb concentration

The DC current has been measured as a function of the DC voltage applied to EPR extruded wire samples at selected temperatures. Although Ohm's Law does not generally hold for dielectrics at high electrical fields, one can still define resistance as $R = V/I$. It then follows that the resistivity of wire insulation is given by

$$\rho = \frac{2\pi L}{\ln(r_2/r_1)} \frac{V}{I} \tag{1}$$

where L is the length of the wire, r_1 the conductor radius, r_2 the insulation radius and $r_1 < r < r_2$. The log resistivity of extruded EPR wire insulations with different Pb concentration, calculated using the measured current (I) and voltage (V) data, has been plotted against mean DC electrical field for the three samples at selected temperatures (Figs 1–3).

It can be seen from Figs 1–3 that the resistivity is electrical field dependent. For all the three wire samples, the electrical field dependence of resistivity is very small at room temperature. At higher temperatures, however, the log resistivity decreases approximately linearly with applied electrical field. The electrical field dependence

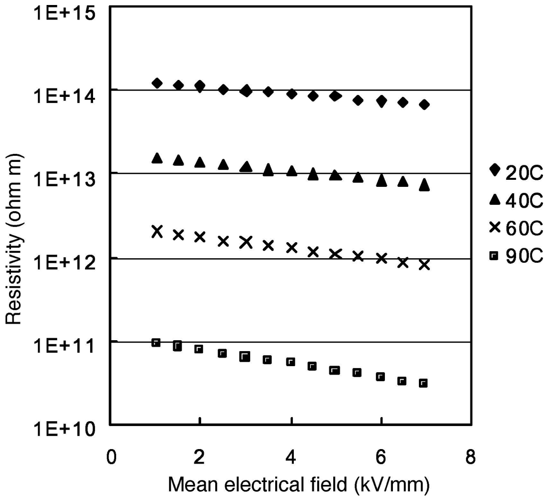

Figure 1 Electrical field dependence of DC resistivity of EPR1 (0 phr Pb) at selected temperatures.

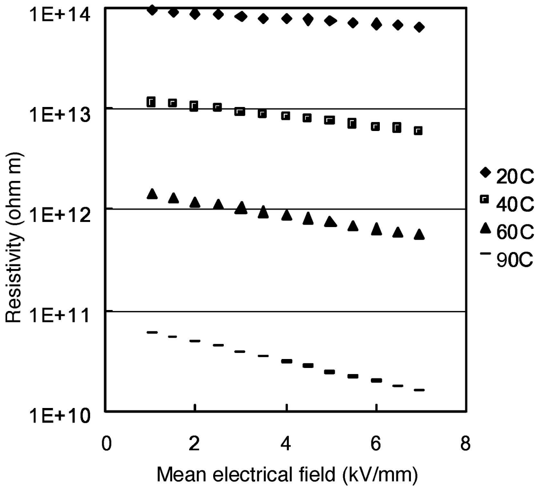

Figure 2 Electrical field dependence of DC resistivity of EPR2 (2.5 phr Pb) at selected temperatures.

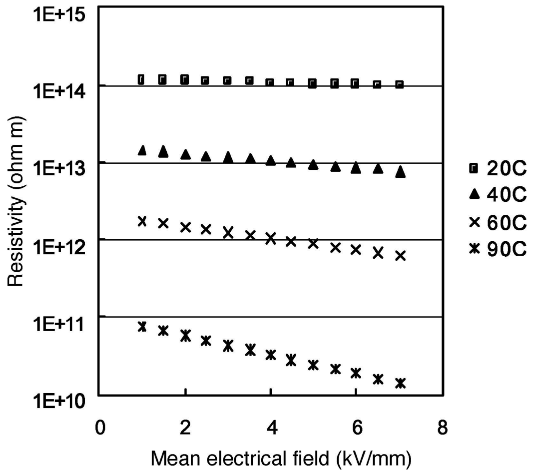

Figure 3 Electrical field dependence of DC resistivity of EPR3 (5 phr Pb) at selected temperatures.

of resistivity can be described by the following equation

$$\rho = \rho_0 \exp(-\beta E) \qquad (2)$$

where E is electrical field, β the electrical field coefficient of resistivity and ρ_0 a constant corresponding to a resistivity at very small electrical field. By fitting a straight line to the log resistivity versus electrical field data, the electrical field coefficient of resistivity, β, can be obtained from the gradient. The results for the three samples with different Pb concentration are given in Table I, together with those for a crosslinked polyethylene (XLPE) sample for comparison [8]. It can be seen that EPR in general has a relatively smaller electrical field coefficient than XLPE and that the electrical field coefficient of EPR increases with temperature while for XLPE it decreases with temperature.

At room temperature, the electrical field coefficient of resistivity of EPR is very small (Table I), indicating that room temperature DC resistivity of EPR is not sensitive to electrical field. At higher temperatures, however, larger values of electrical field coefficient are obtained for the three EPR samples. Moreover, the electrical field coefficient increases with the Pb concentration. This observation may have important technical implications. Since the temperature of the insulation material of a loaded DC cable could be as high as 90°C, the change in electrical field coefficient due to an increase in Pb concentration may affect the electrical field distribution across the cable insulation [9,10].

TABLE I Temperature coefficient α, electrical field coefficient β of DC electrical resistivity for EPR wire insulation EPR1 (no Pb), EPR2 (2.5 phr Pb), EPR3 (5 phr Pb) and XLPE. R-square is the linear regression coefficient

	EPR1	EPR2	EPR3	XLPE [8]
α(K^{-1})	0.101	0.103	0.101	0.099
R-square	0.9980	0.9969	0.9980	0.9210
β (mm/kV) at 20°C	0.096	0.065	0.033	0.83
β (mm/kV) at 90°C	0.189	0.224	0.279	0.42

The results presented in Figs 1–3 also indicate that the resistivity of EPR is strongly temperature dependent and this temperature dependence varies with electrical field. To further highlight the effect of temperature, the resistivity of the three wire insulations has been plotted in Fig. 4 as a function of temperature at a constant electrical field of 0.1 kV/mm. In the temperature ranges studied, the effect of temperature on the resistivity of EPR can best be described by the equation

$$\rho = \rho_{T=0} \exp(-\alpha T) \qquad (3)$$

where T is temperature in Kelvin and α the temperature coefficient of resistivity. The temperature coefficient of resistivity of EPR samples has been obtained by least

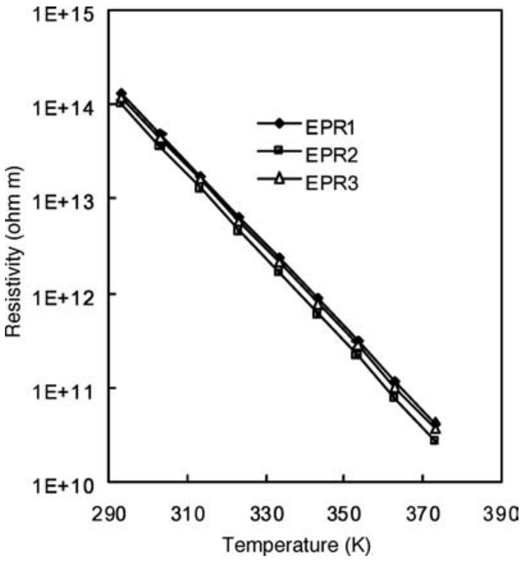

Figure 4 Temperature dependence of DC resistivity for EPR wire insulation materials with different Pb concentrations.

square fitting of the data to a straight line and the results are given in Table I. It can be seen that the temperature coefficients of resistivity of the three EPR samples are approximately the same and independent of Pb concentration. In addition, the temperature coefficient of EPR appears to be similar to that of XLPE (Table I).

3.2. Thermally stimulated discharge current (TSDC)

Before measuring the thermally stimulated discharge current, we have to pole the sample first. EPR sample immersed in tap water was heated to 90°C and then the voltage was ramped up to a value corresponding to an average poling electrical field of 8 kV/mm, at which sample poling was carried out for 120 min while the temperature was kept constant. In the electric field, permanent and induced dipoles orient either individually or under the influence of the motion of neighbouring groups. Thermal motion of the molecules continuously disrupts the orientation of the dipoles in the direction of the applied electric field so that a dynamic equilibrium ensues. Under the influence of the electrical field, charge carriers can also be injected into the sample [11]. These charges migrate to the oppositely charged electrodes and space charge can be built up in their vicinity. After poling the heater was turned off and the sample was left to cool down to room temperature under the highest electrical field (8 kV/mm).

In general, TSDC gives information on dipole relaxation, charge injection and detraping processes in electrical insulation materials [11]. After poling (stressing) at the highest voltage and temperature, all the dipoles are lined up with the electrical field and their contribution to the DC current tends to be zero. The current measured now includes only the contribution from charge carriers, whether they are injected or activated from traps. Therefore, the temperature dependence of DC current under constant voltage will lead to a determination of trap depth.

According to theory, the space charge limited current density J that flows for an applied voltage V can be given by the Mott and Gurney square law [12]

$$J = \frac{9\varepsilon_0 \varepsilon_r V^2}{8L^2}\theta \tag{4}$$

where L is sample thickness and

$$\theta = \frac{n_c}{n_t} = \frac{N_{\text{eff}}}{N_t}\exp\left(-\frac{\Delta E_t}{kT}\right) \tag{5}$$

is the ratio of free charge carriers to those trapped. In Equation 5, n_c and n_t are the densities of free charge carriers and trapped carriers respectively, N_t is the number density of traps with trap depth ΔE_t (an energy below the bottom of the conduction band) and N_{eff} the effective density of states for the conduction band. Now, if Equation 5 were correct, an Ln DC current versus $1/T$ plot would result in a straight line, which is exactly what we can see in Fig. 5. From the gradient of the straight line, the trap depth ΔE_t has been calculated for the three EPR samples. The results are given in Table II. Note that the band gap of polyethylene is 8.8 eV and we would assume a similar value for EPR formulation. The trap depth of EPR is slightly larger than that of XLPE (0.990 eV) [8]. Note that the experimental data in Fig. 5 have been obtained under constant voltage after poling" and therefore is a direct consequence of long-range migration of charge carriers. This is rather different from the data given in Fig. 4, which include contributions from both charge carriers and dipole reorientation. It is evident from Fig. 5 that Pb doping introduces more charge carriers and therefore increases the conductivity of the EPR materials. However, Pb particles may also result in an increase in the number of traps that would subsequently decrease the conductivity. Moreover, increasing the Pb concentration could reduce the mobility of the molecular dipoles, which will also lead to an increase in resistivity. The competition of theses effects determines the electrical properties of the EPR samples and might be partially responsible to the resistivity data presented in Fig. 4.

After the sample temperature reached the room temperature, the applied DC voltage was turned off and the

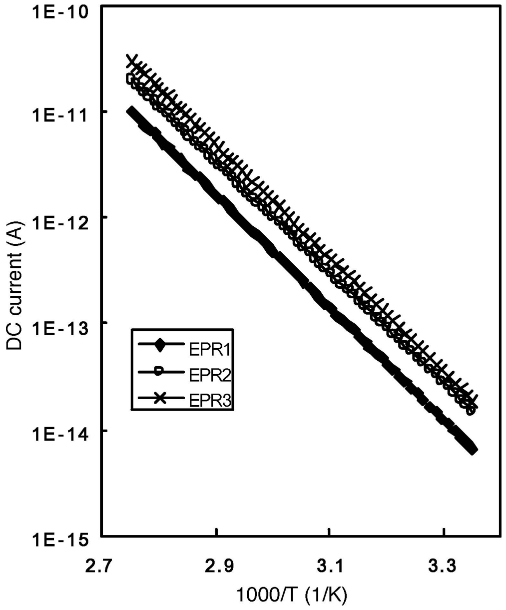

Figure 5 Temperature dependence of DC current for EPR materials at a constant electrical field of 8 kV/mm. The data were obtained when the samples were cooled down to room temperature after poling.

TABLE II TSDC peak position T_p, peak height I_p and trap depth ΔE_t for extruded EPR wire insulation with different Pb concentration

	EPR1	EPR2	EPR3
T_p (°C)	79	85	83
I_p (pA)	641	523	623
ΔE_t (eV)	1.054 ± 0.005	1.037 ± 0.005	1.064 ± 0.005

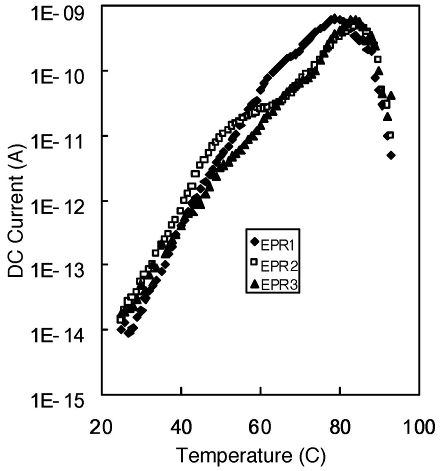

Figure 6 Temperature dependence of TSDC current for EPR samples with different Pb contents.

sample was short circuited and discharged for ∼12 h. To measure the thermally stimulated discharge current, the sample short circuited across the Keithley electrometer, was heated linearly up to 93°C with a heating rate of ∼1°C/min. An external collecting voltage up to 130 V did not have any detectable effect on the discharge current. The sign of the current remained the same even if the polarity of the external collecting voltage was changed. The flow of the activated carriers is mainly controlled by the local field due to trapped charges in the vicinity of electrodes. For this reason, no collecting voltage was applied during the TSDC test.

It was observed that the direction of the current flow during the TSDC measurements is always consistent with that of a normal discharge current, indicating that the trapped space charge in EPR wire insulation is homocharge. The TSDC spectra of the three EPR wire insulations are given in Fig. 6. The spectrum consists of mainly a broad positive peak (i.e. the current flow is in the normal discharge direction), with a shoulder somewhat 20°C below the main peak. The peak height and peak temperature of the three samples are also listed in Table II. Although the discharge current includes contributions from both charge carriers and dipoles, the main feature of the spectrum arises from orientational relaxation of the dipoles within the insulation. The physical origin of the shoulder might be well associated with the order-disorder transition of EPR at ∼60°C, evidenced by ultrasonic measurements [13], where a pronounced change of slope in the temperature dependence of longitudinal wave velocity was observed. In addition this feature in the TSDC spectrum seems to be correlated with the sharp drop in logG' and a peak in tanδ observed at 40°C in the dynamic mechanical thermal analysis (DMTA) test [13, 14].

While features at lower temperatures can be associated with conventional mechanical processes, the main TSDC peak that occurs well above the glass transition temperature (about –60°C [3–5]) must correspond to the release of charge carriers from electron traps and can only be investigated using TSDC technique. TSDC peak height is a measure of the density of trapped carriers and frozen dipoles in the poled material. It can be seen from Table II that the peak height for sample EPR2 with 2.5 phr Pb is the lowest. This means that fewer charges were trapped and fewer dipoles were frozen in the insulation during the poling. The data presented in Table II indicate that more charges will be trapped in the insulation if the traps are deeper. In any case, the releasing of charges, whether they are trapped carriers or frozen dipoles, seems to be dominantly controlled by the molecular motion in the polymer.

TSDC peak temperature T_p is directly related to the electron trap depth: while charge carriers in shallow traps can be released at low temperatures, higher temperature is needed to activate the charges in deep traps. The broad TSDC peak observed for the three EPR samples indicates that there is a distribution in the trap depth. Some of the traps are shallow and some of them are deep. The space charge limited conduction model used in the previous section is over simplified and the trap depth obtained there is only an average over traps of various depths. The fact that lead doping shifts the TSDC peak to higher temperatures suggests that deeper traps have been introduced.

4. Conclusion

To summarise, the DC resistivity of 3 extruded EPR samples with different Pb concentration have been measured under wet conditions as a function of electrical field at selected temperatures up to 100°C. The temperature and electrical field coefficients of resistivity have been determined. Based on a space charge limited conduction model, the trap depth has been obtained for the three EPR samples. TSDC test has also been made and a broad positive peak has been observed. It has been shown that the resistivity of EPR is not sensitive to Pb concentration in the range of 0 to 5 phr. The temperature coefficient of resistivity α of EPR has been measured to be ∼0.1 K^{-1} for all the samples with various Pb concentration. The electrical field coefficient of resistivity β of EPR increases with temperature and is smaller than that for XLPE. Increasing Pb content increases slightly the electrical field coefficient of resistivity, which may have important technical implications for cable applications. TSDC measurements show that doping with Pb increases both the density of charge carriers and number of deep traps simultaneously. The broad TSDC peak suggests that there must be a distribution in the trap depth rather than just a single value.

References

1. R. N. HAMPTON, F. CHANG and S. B. HOBDELL, CIGRE Session 2000, P2-001.
2. V. BUCHHOLZ, "Finding the Root Cause of Power Cable Failures" (Electric Energy Publications Inc., 2004) http://www.jaguar-media.com/english.
3. R. KARPELES and A. V. GROSSI, "EPDM rubber technology," Handbook of Elastomers, 2nd edn., edited by A. K. Bhowmick and H. L. Stephens (Marcel Decker, Inc., New York, 2001) p. 845.

4. J. A. RIEDEL and R. V. LAAN, "Ethylene Porpylene Rubbers," The Vanderbilt Rubber Handbook 13th edn. (R.T. Vanderbilt Co., Inc., Norwalk, CT, 1990) p. 123.
5. G. V. STRATE, Ethylene Propylene Elastomers, vol. 6 (Encyclopedia of Polymer Science & Engineering, 1986) p. 522.
6. N. CHIWATA, "Deterioration characteristics of rubber insulation materials subjected to electrical stress under water immersion," *Nippon Gomu Kyokaishi*, **76**(4) (2003) 129 (General Review in Japanese).
7. L. HARRIMAN, "Environmental, health and safety issues in the coated wire and cable industry," Technical Report No. 51 April 2002 University of Massachusetts Lowell. Website: http://www.turi.org/content/content/download/913/4501/file/Wire_Cable_TechReport.pdf.
8. F. CHANG, Manuscript for the 14th International Symposium on High Voltage Engineering, in preparation.
9. B. ALADENIZE, R. COELHO, J. C. ASSIER, H. JANAH and P. MIREBEAU, Jicable'99 (1999) p. 557.
10. F. CHANG, R. N. HAMPTON and S. B. HOBDELL, in Jicable'99 (1999) p. 685.
11. G. KAMPF, "Characterization of Plastics by Physical Methods" (Hanser Publishers, Munich Vienna, New York, 1986).
12. J. C. FOTHERGILL and L. A. DISSADO, in "Electrical Degradation and Breakdown in Polymers" (Peter Perigrinus Publishing, London, 1992).
13. C. FANGGAO, G. A. SAUNDERS, E. F. LAMBSON and R. N. HAMPTON, in Proceedings of the International Conference on Electrical, Optical and Acoustic Properties of Polymers EOA III (The institution of Civil Engineers, Great George Street, Westminster, London SW1P, 16–18th September 1992).
14. C. FANGGAO, University of Bath M. Phil. thesis (1992).

Received 20 February
and accepted 26 May 2005